ISSN: 2754-4966

Journal of Nanosciences Research & Reports

SCIENTIFIC Research and Community

Research Article

Open Access

Chitosan Sulfate Nanoparticles Synthesis and Characterization from Penaeus Monodon Exoskeleton

Langston N Forbes Jackson[1], Nithin Krisshna Gunasekaran[1], Krishnan Prabhakaran[1], Joseph C Hall[1], Singaram Muthukaruppan[2] and Govindarajan T Ramesh[1]*

[1]Center for Materials Research/Biology, Norfolk State University, 700 Park Avenue, Norfolk VA, 23504, USA

[2]Poseidon Biotech, Chennai, TN 600085, India

ABSTRACT

Chitosan was extracted from shrimp shell biowaste through a sequential three-step process of deproteinization, demineralization, and deacetylation, yielding a high-degree-of-deacetylation chitosan precursor that was subsequently sulfated and formulated into nanoparticles. Physicochemical characterization was performed using a complementary suite of analytical techniques: Fourier transform infrared spectroscopy (FTIR) confirmed the structural integrity of the chitosan, field emission scanning electron microscopy (FESEM) with energy-dispersive X-ray spectroscopy (EDS) revealed a rough, porous, and interconnected nanoparticulate morphology, and X-ray diffraction (XRD) confirmed the crystalline structure of chitosan. Biocompatibility assessment conducted using the MTT assay on BEAS-2B human bronchial epithelial cells demonstrated that the nanoparticles maintain cell viability above 90% at low to moderate concentrations. These results collectively establish that shrimp shell waste is a viable sustainable precursor to produce chitosan sulfate nanoparticles with confirmed chemical identity, appropriate nanoscale morphology, and favorable biocompatibility, supporting their further development for drug delivery, antiviral, anticoagulant, and tissue engineering applications.

***Corresponding author**

Govindarajan T Ramesh, Norfolk State University 700 Park Avenue, Norfolk VA, 23504, USA.

Received: June 19, 2026; **Accepted:** June 23, 2026; **Published:** July 30, 2026

Keywords: Nanoparticle Synthesis, Chitosan Sulfate, Chitosan, Biomaterials, Drug Delivery Systems

Introduction

Chitosan sulfate nanoparticles (CS-NPs) represent a chemically modified class of biopolymeric nanomaterials derived from chitosan, a linear aminopolysaccharide composed of β-(1→4)-linked D-glucosamine and N-acetyl-D-glucosamine units produced by the alkaline deacetylation of chitin [1]. Unlike native chitosan, which carries a cationic character due to free amine groups at the C-2 position, sulfation introduces anionic sulfate moieties (SO_3H or SO_3^-) onto the hydroxyl and amino functionalities at the C-2, C-3, and C-6 positions of the glucosamine backbone, transforming the polymer into a polyanionic or zwitterionic structure depending on the degree of substitution (DS) [2]. This structural transformation imparts heparin-like physicochemical properties, including enhanced water solubility at neutral and alkaline pH, increased bioactivity, and functional similarity to heparan sulfates, naturally occurring glycosaminoglycans that play pivotal roles in cell signaling, growth factor binding, and viral attachment [3]. The degree of sulfation, typically ranging from 0.3 to 2.0 sulfate groups per monosaccharide unit, critically governs the biological efficacy, solubility, thermal stability, and surface charge characteristics of the resulting nanoparticles [4].

The conventional synthesis of chitosan sulfate and its subsequent nanoparticle formation involves two sequential stages, chemical sulfation of the chitosan backbone followed by nanoparticle assembly [5]. Chemical sulfation is most commonly achieved using the chlorosulfonic acid-oleum method, wherein chitosan is treated with a complex of chlorosulfonic acid ($ClSO_3H$) and fuming sulfuric acid in amide solvents such as N-dimethylformamide (DMF) or dimethylsulfoxide (DMSO), yielding sulfated chitosan with anticoagulant, antiviral, and antisclerotic activities [6]. A more selective C-6 sulfation route employs a mixture of H_2SO_4 and $ClSO_3H$ at controlled ratios and temperatures, producing chitosan-6-sulfate with well-defined single sulfate groups per glucosamine unit and enhanced structural specificity for pharmaceutical applications [7]. For other approaches, the SO_3-pyridine complex has been employed for regioselective sulfation, with N-sulfation or O-sulfation achieved depending on the protection strategy and reaction medium, including the use of ionic liquids such as 1-butyl-3-methylimidazolium chloride (BMImCl) to achieve homogeneous sulfation and minimize depolymerization [8]. Once sulfated, nanoparticles are most commonly assembled by ionic gelation, in which the anionic sulfate groups of the chitosan sulfate participate in polyelectrolyte complexation with oppositely charged species or serve as self-crosslinking sites [9]. Additional methods include polyelectrolyte complexation with cationic polymers, nanoprecipitation, and spray-drying, each offering

distinct advantages in terms of particle size control, encapsulation efficiency, and scalability [10].

The unique heparin-mimicking properties of chitosan sulfate nanoparticles have established them as highly versatile platforms across a broad spectrum of biomedical applications [11]. In the field of antiviral therapeutics, synthetic chitosan sulfate derivatives functioning as Heparan Sulfate Proteoglycan (HSPG) mimics have demonstrated broad-spectrum activity against SARS-CoV-2, Respiratory Syncytial Virus (RSV), HIV, herpes simplex virus, and human papillomavirus, primarily by binding viral surface glycoproteins and blocking host cell attachment and membrane fusion [12]. Furthermore, chitosan sulfate nanoparticles are actively explored in tissue engineering including bone morphogenetic protein (BMP-2)-mediated osteogenesis, cartilage scaffold fabrication, and vascular graft construction by mimicking the glycosaminoglycan-rich extracellular matrix environment and modulating growth factor signaling [13]. In drug delivery systems, their mucoadhesive properties, stimuli-responsive release behavior at tumor microenvironment pH, and surface modifiability enable efficient loading and targeted delivery of chemotherapeutic agents, genes, and vaccine antigens [14].

A growing and sustainable route to chitosan sulfate nanoparticles begins with the biosynthetic extraction of chitosan directly from seafood processing waste, particularly shrimp shell waste which is among the most abundant and underutilized bio-waste streams globally [15]. The extraction process follows three sequential stages: demineralization, wherein dried and powdered shrimp shells are treated with dilute hydrochloric acid (typically 1.3–5% HCl) to remove calcium carbonate mineral content [16]. Deproteinization, involves alkaline treatment with NaOH solution (2–12 N) at elevated temperatures (50–80°C) to solubilize and remove structural proteins, yielding chitin and deacetylation, in which chitin is treated with concentrated NaOH (12–50%) under controlled temperature and duration to remove acetyl groups and produce chitosan with degrees of deacetylation (DDA) typically ranging from 75% to 90% [17]. The waste-derived chitosan is then subjected to the sulfation reactions described above to produce chitosan sulfate, which is subsequently formulated into nanoparticles via ionic gelation or polyelectrolyte self-assembly [18]. One of the published studies confirms that shrimp shell-derived chitosan exhibits FTIR spectral profiles and degrees of deacetylation comparable to commercially sourced chitosan, with physicochemical attributes that directly influence nanoparticle size, zeta potential, and biological activity [19]. Importantly, low molecular weight sulfated chitosan (LMWSC) has also been extracted directly from cephalopod shell waste (Sepia species) through a combined de-amination, deproteinization, deacetylation, and sulfation protocol, confirmed neuroprotective and antiviral activities [20].

The valorization of shrimp and broader seafood shell waste for the biosynthesis of chitosan sulfate nanoparticles carries substantial environmental, economic, and societal significance within the framework of circular bioeconomy principles [21]. The global seafood industry generates enormous quantities of shell waste. Redirecting this waste stream toward the recovery of chitin, chitosan, and derived sulfated nanoparticles transforms what is otherwise an environmental liability into high-value bioactive materials, thereby reducing disposal costs, cutting emissions, and creating revenue through bioproduct sales, a classic biorefinery model embedded within blue economy frameworks [22]. A 2020 review published in Environmental Pollution (Elsevier) underscored the concerted shift from harsh chemical strategies toward enzymatic, microbial, and mild physical processing techniques for shrimp shell valorization, reducing the environmental burden of acid and alkali effluents associated with conventional demineralization and deproteinization [23]. More broadly, the convergence of green synthesis, seafood waste valorization, and nanotechnology enables the development of sustainable biomedical materials that close the loop between marine food processing industries and pharmaceutical innovation, connecting coastal communities, waste management infrastructure, and advanced materials science [24]. This paradigm aligns with the United Nations Sustainable Development Goals and positions chitosan sulfate nanoparticles from seafood waste not merely as functional nanomaterials, but as embodiments of responsible, circular material design relevant to researchers working at the intersection of sustainable chemistry, nanomedicine, and environmental engineering [25].

Materials and Methods

Synthesis of Chitosan Sulfate Nanoparticles

The synthesis of chitosan from shrimp shell waste in this work follows the three-step chemical route of deproteinization, demineralization, and deacetylation that is widely reported for crustacean biowaste valorization into chitin and chitosan [26]. In the first step, deproteinization, thoroughly washed and dried shrimp waste is crushed and treated with 4% NaOH under continuous stirring for 24 hours, where the alkaline medium breaks peptide bonds and solubilizes proteins and lipids; repeated washing with deionized water to neutral pH removes dissolved organics and excess alkali, leaving a protein-free solid residue [27]. This residue is then subjected to demineralization by soaking in 4% HCl for 12 hours, during which calcium carbonate and other mineral salts dissolve and are removed; filtration and rinsing with deionized water yield purified chitin, consistent with acid demineralization conditions commonly used for shrimp and prawn shells. In the final deacetylation step, the chitin is treated with concentrated 50% NaOH for 3 days with continuous stirring, allowing alkaline hydrolysis of N-acetyl groups at the C-2 position of the glucosamine units and converting them to free amino groups, thus producing chitosan with a high degree of deacetylation suitable for further nanoparticle formulation. The obtained chitosan is then dried at 60°C to remove residual moisture and stored at room temperature, providing a stable biopolymer precursor for subsequent nanoparticle synthesis via standard methods such as ionic gelation or polyelectrolyte complexation.

FTIR Analysis

Fourier Transform Infrared (FTIR) spectra of the samples were recorded using a Thermo Scientific Nicolet iS50 spectrometer equipped with an Attenuated Total Reflectance (ATR) accessory. The analysis was conducted in the mid-infrared region from 4000 to 500 cm^{-1}, which covers the principal vibrational modes of chitosan and its sulfate functional groups. For each measurement, the finely ground powder was placed directly onto the ATR crystal, and gentle pressure was applied with the built-in pressure arm to ensure intimate contact between the sample and the crystal surface, thereby maximizing signal quality and minimizing spectral artefacts due to poor optical coupling [28]. A background spectrum was collected prior to each sample run under the same conditions, and all spectra were recorded at room temperature with an appropriate spectral resolution and number of scans to improve the signal-to-noise ratio [29]. The ATR configuration eliminates the need for KBr pellets or other dispersive media, reduces sample preparation time, and allows direct analysis of powders, making it well suited for routine characterization and comparison of chitosan, sulfated chitosan, and nanoparticle formulations [30].

FESEM Analysis

Field Emission Scanning Electron Microscopy (FESEM) was conducted using a Hitachi S 4700 instrument equipped with an Energy Dispersive X Ray Spectroscopy (EDS) detector to characterize both the morphology and elemental composition of the chitosan sulfate nanoparticles. A clean aluminum stub was first covered with conductive carbon tape, and a well dispersed, sonicated nanoparticle suspension was drop cast onto the tape and dried overnight at room temperature to obtain a thin, uniform layer that minimized severe aggregation [31]. The dried stub was then loaded into the FESEM chamber and imaged under high vacuum using an appropriate accelerating voltage and working distance to achieve high surface resolution while limiting beam damage to the organic matrix [32]. Secondary electron imaging was employed to reveal surface roughness, particle shape and agglomeration behavior, and selected areas were analyzed by EDS to confirm the expected elemental signals and to check for unwanted contaminants [33]. This combination of careful sample preparation and optimized FESEM/EDS conditions ensured reliable visualization of the chitosan nanoparticle microstructure together with supporting compositional information.

XRD Analysis

X-ray Diffraction (XRD) analysis of the chitosan sulfate nanoparticles was performed using a PANalytical Empyrean Series 2 X-ray diffraction system. The finely ground powder was loaded directly onto the sample holder and mounted in the diffractometer, and the diffraction pattern was collected over a 2θ scan range appropriate for identifying the crystalline phases present in the material [34]. The instrument uses Cu Kα radiation as the X-ray source, and the diffraction data are collected as a function of diffraction angle (2θ), where constructive interference occurs according to Bragg's law when the incident beam wavelength matches the interplanar spacing of lattice planes in the material [35]. The direct powder-loading approach minimizes sample preparation time and is suitable for powdered nanomaterials, ensuring that the observed diffraction pattern reflects the bulk-phase composition of the nanoparticles without interference from mounting media.

MTT Assay

The cytotoxicity of the chitosan sulfate nanoparticles was evaluated using the 3-(4,5-dimethylthiazol-2-yl)-2,5-diphenyltetrazolium bromide (MTT) colorimetric assay, which quantifies cell viability based on the metabolic activity of living cells [36]. On Day 1, BEAS-2B human bronchial epithelial cells were seeded in a 96-well plate at an appropriate cell density in complete growth medium and incubated for 48 hours at 37°C in a humidified 5% CO_2 atmosphere to allow the cells to adhere and reach a sub-confluent monolayer. Following this initial incubation, the culture medium was replaced with fresh medium containing chitosan sulfate nanoparticles at a range of concentrations (1, 2, 5, 10, 15, 25, 50, 75, and 100 µg/mL), alongside an untreated negative control (NC), and the cells were incubated for a further 48 hours under the same conditions. After treatment, the medium was removed and a freshly prepared MTT dye solution (typically 0.5 mg/mL in phosphate-buffered saline) was added to each well and incubated for 3–4 hours. During this process, the yellow MTT reagent is reduced by mitochondrial dehydrogenase enzymes in metabolically active cells to form insoluble purple formazan crystals and the amount of formazan produced is directly proportional to the number of viable cells [37]. The formazan crystals were then dissolved by adding a solubilization reagent such as DMSO, and the absorbance of each well was measured using a microplate spectrophotometer at 570 nm [38]. The percentage cell viability for each treatment group was calculated relative to the negative control, which was set as 100% viability. Single walled carbon nanotubes (SWCNTs) were used as a positive control, given their well-documented cytotoxicity.

Results and Discussion

FESEM Analysis

The FESEM image in Figure 1 shows a continuous chitosan surface prior to sulfation, composed of many interconnected, flake like domains that form a dense three dimensional network. The morphology is clearly non spherical and is characterized by wrinkled flakes, folds and ridges, together with several dark regions that correspond to interconnected pores and voids within the coating. This gives the surface a uniform micro rough and moderately porous texture, which increases the effective surface area and can improve adhesion, adsorption and potential drug loading behavior. The absence of large cracks or delaminated regions indicates that the coating is mechanically coherent and well consolidated over the substrate. The accompanying EDS spectrum shows intense peaks for carbon and oxygen, confirming that the observed region is dominated by an organic polysaccharide matrix consistent with chitosan. Together, the FESEM and EDS results indicate a homogeneous chitosan layer with a rough, porous microstructure and a clean elemental composition.

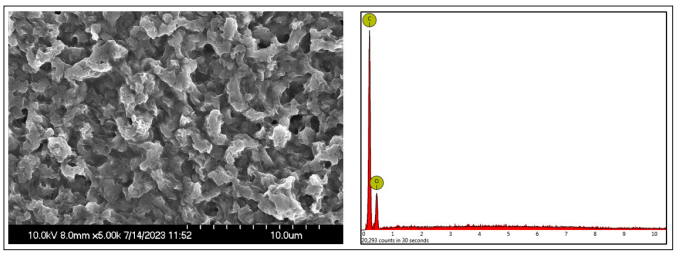

Figure 1: FESEM Image of Chitosan Nanoparticles with EDS Spectra

FTIR Analysis

The FTIR spectrum of the chitosan sulfate nanoparticles in Figure 2 shows the characteristic vibrations of a sulfated chitosan backbone, confirming successful sulfation and nanoparticle formation. The broad band at 3000–3500 cm^{-1} arises from overlapping O-H and N-H stretching of hydroxyl groups and primary amines in the glucosamine units, while the weaker bands at 2920-2880 cm^{-1} correspond to aliphatic C-H stretching of CH_2 and CH groups in the polysaccharide ring [39]. In the amide region, the strong band near 1640-1600 cm^{-1} is attributed to amide I C=O stretching of residual N-acetyl groups together with N-H bending of protonated NH_2 groups, and the band around 1550 cm^{-1} to amide, both commonly used to track chitosan deacetylation and modification [40]. The most diagnostic sulfation features appear in the fingerprint region, a band at 1230–1270 cm^{-1} due to asymmetric S=O stretching and a distinct band at 800 to 830 cm^{-1} assigned to C-O-S bending, which are widely recognized as markers of sulfate ester groups on chitosan. The strong band system between about 1150 and 1000 cm^{-1}, dominated by glycosidic C-O stretching [41]. Together, these features demonstrate that the material is chitosan sulfate in nanoparticulate form, in good agreement with published FTIR assignments for sulfated chitosan.

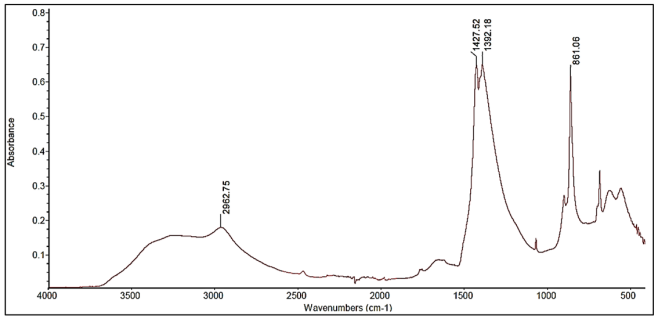

Figure 2: FTIR Spectra of Chitosan Sulfate Nanoparticles

XRD Analysis

The XRD pattern of the nanoparticle sample in Figure 3 displays five distinct diffraction peaks indexed to the (2,2,0), (3,1,1), (4,0,0), (4,2,2), and (4,4,0) crystallographic planes, with the most intense peak appearing at the (4,0,0) reflection at approximately $2\theta \approx 45°$. This set of reflection conditions where the sum of Miller indices h, k, and l is even is characteristic of a face-centered cubic (FCC) spinel crystal structure, consistent with the crystal structure of magnetite (Fe_3O_4) as confirmed by JCPDS card No. 19-0629 and widely reported in published literature for magnetic nanoparticle systems. The presence of these well-defined sharp peaks confirms the crystalline nature of the inorganic component incorporated into the chitosan sulfate matrix, indicating successful synthesis of a chitosan sulfate nanocomposite. The relatively sharp and distinct peak profiles suggest a reasonable degree of long-range crystalline order in the Fe_3O_4 phase, while the absence of additional sharp peaks from the chitosan sulfate component is expected, as chitosan is inherently semi-crystalline to amorphous and typically produces only broad, low-intensity humps rather than sharp reflections.

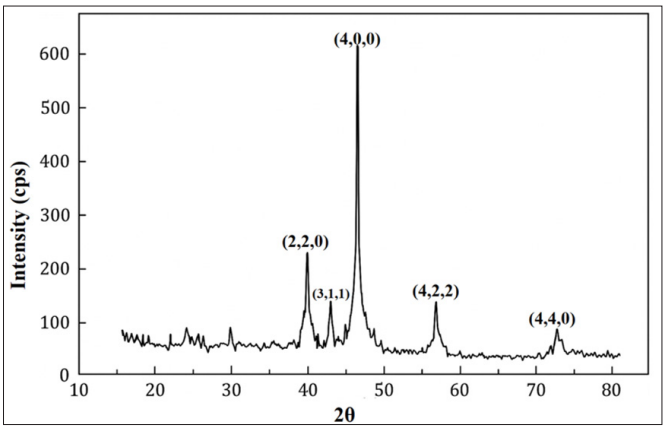

Figure 3: XRD Spectra of Chitosan Sulfate Nanoparticles

MTT Assay

The MTT assay results in Figure 4 indicate that chitosan sulfate nanoparticles are well tolerated by Beas 2B cells at lower and intermediate doses but begin to show a concentration dependent reduction in viability at higher doses. Cell viability remains close to that of the negative control (NC) at 1–5 µg/µL, indicating negligible cytotoxicity in this range. A gradual decline is then observed as the concentration increases from 10 to 100 µg/µL, viability drops to around 90% at 10-25 µg/µL, to approximately 75-80% at 50-75 µg/µL, and further to about 70% at 100 µg/µL. This trend suggests the onset of mild to moderate cytotoxic effects only at the highest concentrations. In contrast, the SWCNT positive control (PC) shows a pronounced reduction in viability to roughly 15-20%, confirming that the assay is capable of detecting strong cytotoxic responses and highlighting that the effects of chitosan sulfate nanoparticles are comparatively modest. Overall, the analysis support that chitosan sulfate nanoparticles are largely biocompatible toward Beas 2B cells till the nanoparticle concentration of 25 µg/µL, with only concentration dependent, partial reductions in viability at higher doses.

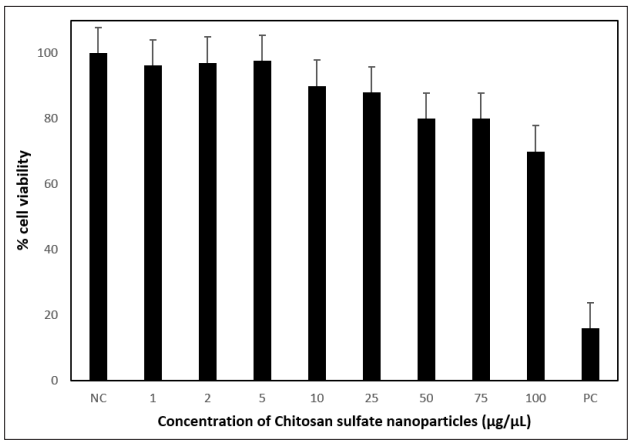

Figure 4: MTT Assay Results of Chitosan Sulfate Nanoparticles

Conclusion

In conclusion, this study successfully demonstrated the biosynthesis of chitosan sulfate nanoparticles from shrimp shell waste through a sequential deproteinization, demineralization, and deacetylation process followed by chemical sulfation. FESEM imaging revealed a rough, porous, and interconnected nanoparticulate morphology, while EDS confirmed the organic elemental composition consistent with a chitosan matrix free from inorganic contaminants. FTIR spectral analysis confirmed the structural integrity of the chitosan backbone and the covalent incorporation of sulfate ester groups, as evidenced by the characteristic S=O stretching and C–O–S bending vibrations in the fingerprint region. XRD analysis further supported the crystalline character of the inorganic phase incorporated within the nanocomposite. Importantly, the MTT assay using BEAS-2B cells demonstrated that the chitosan sulfate nanoparticles are largely biocompatible at low to moderate doses (1–25 µg/µL), with only mild, concentration-dependent reductions in cell viability observed at higher concentrations. Collectively, these findings establish that shrimp shell waste is a viable and sustainable precursor for the green synthesis of chitosan sulfate nanoparticles with confirmed chemical identity, appropriate nanoscale morphology, and acceptable biocompatibility, supporting their further development as functional nanomaterials for biomedical applications.

Acknowledgement

The authors would like to thank the Center for Molecular Diagnostics & Next Generation Sequencing, Norfolk State University.

References

1. Jhaveri J, Raichura Z, Khan T, Momin M, Omri A (2021) Chitosan nanoparticles-insight into properties, functionalization and applications in drug delivery and theranostics. Molecules 26: 272.
2. Chicea D, Nicolae-Maranciuc A (2024) A review of chitosan-based materials for biomedical, food, and water treatment applications. Materials 17: 5770.
3. Revuelta J, Fraile I, Monterrey DT, Pena N, Benito-Arenas R, et al. (2021) Heparanized chitosans: Towards the third generation of chitinous biomaterials. Mater Horiz 8: 2596-2614.

4. Zhang B, Yang X, Li P, Guo C, Ren X, et al. (2018) Preparation of chitosan sulfate and vesicle formation with a conventional cationic surfactant. Carbohydr Polym 183: 240-245.
5. Fatoni A, Ahmad IN, Utami H, Erjon, Rendowaty A, et al. (2023) Synthesis, characterization of chitosan sulfate nanoparticles and their activity against bacterial. AIP Conf Proc 2913: 020007.
6. Al-Remawi MM (2012) Properties of chitosan nanoparticles formed using sulfate anions as crosslinking bridges. Am J Appl Sci 9: 1091-1100.
7. Zhang C, Zhang H, Li R, Xing Y (2017) Morphology and adsorption properties of chitosan sulfate salt microspheres prepared by a microwave-assisted method. RSC Adv 7: 48189-48198.
8. Kocabay S, Bahar MR, Tekin S, Akkaya R, Akkaya B (2021) Chemical and biological characterization of sulfated chitosan oligomer as heparin mimics. Polym Polym Compos 29: S1023-S1032.
9. Erasov VS, Maltseva YO (2024) Obtaining chitosan sulfate nanoparticles in an aqueous medium and their colloidal protection with polysaccharides. Fine Chem Technol 19: 111-126.
10. Anand M, Sathyapriya P, Maruthupandy MA, Beevi AH (2018) Synthesis of chitosan nanoparticles by TPP and their potential mosquito larvicidal application. Front Lab Med 2: 72-78.
11. Chicea D, Nicolae-Maranciuc A (2024) A review of chitosan-based materials for biomedical, food, and water treatment applications. Materials 17: 5770.
12. Song W, Zeng Q, Yin X, Zhu L, Gong T, et al. (2018) Preparation and anticoagulant properties of heparin-like electrospun membranes from carboxymethyl chitosan and bacterial cellulose sulfate. Int J Biol Macromol 120: 1396-1405.
13. Tan RS, Hassandarvish P, Chee CF, Chan LW, Wong TW (2022) Chitosan and its derivatives as polymeric anti-viral therapeutics and potential anti-SARS-CoV-2 nanomedicine. Carbohydr Polym 290: 119500.
14. Bolshakov IN, Gornostaev LM, Fominykh OI, Svetlakov AV (2022) Synthesis, chemical and biomedical aspects of the use of sulfated chitosan. Polymers 14: 3431.
15. Rajkumar DS, Keerthika K, Vijayaragavan V (2024) Chitosan-based biomaterial in wound healing: A review. Cureus 16: e55189.
16. Grewal AK, Salar RK (2024) Chitosan nanoparticle delivery systems: An effective approach to enhancing efficacy and safety of anticancer drugs. Nano TransMed 3: 100040.
17. Teixeira-Costa BE, Andrade CT (2021) Chitosan as a valuable biomolecule from seafood industry waste in the design of green food packaging. Biomolecules 11: 1599.
18. Hosney A, Ullah S, Barčauskaitė K (2022) A review of the chemical extraction of chitosan from shrimp wastes and prediction of factors affecting chitosan yield by using an artificial neural network. Mar Drugs 20: 675.
19. Zhang C, Zhang H, Li R, Xing Y (2017) Morphology and adsorption properties of chitosan sulfate salt microspheres prepared by a microwave-assisted method. RSC Adv 7: 48189-48198.
20. Ahmed HA, El-Maradny YA, Shalaby MA, El-Menshawy H, Abd El-Wahab AE (2025) Isolation and characterization of chitosan from shrimp shell waste and the sustainable preparation of salicylic acid-loaded chitosan nanoparticles for antibiofilm applications. Sci Rep 15: 19263.
21. Doncel-Pérez E, Aranaz I, Bastida A, Revuelta J, Camacho C, Acosta N, et al. (2018) Synthesis, physicochemical characterization and biological evaluation of chitosan sulfate as heparan sulfate mimics. Carbohydr Polym 191: 225-233.
22. Mathew GM, Mathew DC, Sukumaran RK, Sindhu R, Huang CC, et al. (2020) Sustainable and eco-friendly strategies for shrimp shell valorization. Environ Pollut 267: 115656.
23. Zulkarnain Z, Mukti WA, Kurniawan K (2024) Sustainable and environment-friendly management of shrimp processing waste through high-quality chitosan production. Leuser J Environ Stud 2: 95-100.
24. Teixeira-Costa BE, Andrade CT (2021) Chitosan as a valuable biomolecule from seafood industry waste in the design of green food packaging. Biomolecules 11: 1599.
25. Frigaard J, Jensen JL, Galtung HK, Hiorth M (2022) The potential of chitosan in nanomedicine: An overview of the cytotoxicity of chitosan-based nanoparticles. Front Pharmacol 13: 880377.
26. Hosney A, Ullah S, Barčauskaitė K (2022) A review of the chemical extraction of chitosan from shrimp wastes and prediction of factors affecting chitosan yield by using an artificial neural network. Mar Drugs 20: 675.
27. Pakizeh M, Moradi A, Ghassemi T (2021) Chemical extraction and modification of chitin and chitosan from shrimp shells. Eur Polym J 159: 110709.
28. Rehman HU, Cord-Landwehr S, Shapaval V, Dzurendova S, Kohler A, et al. (2023) High-throughput vibrational spectroscopy methods for determination of degree of acetylation for chitin and chitosan. Carbohydr Polym 302: 120428.
29. Doğan M (2020) Preparation of chitosan nanoparticles and characterization studies. Cumhuriyet Med J 42: 1-10.
30. Fatoni A, Ahmad IN, Utami H, Erjon, Rendowaty A, Hidayati N (2023) Synthesis, characterization of chitosan sulfate nanoparticles and their activity against bacterial. AIP Conf Proc 2913: 020007.
31. Khanmohammadi M, Elmizadeh H, Ghasemi K (2015) Investigation of size and morphology of chitosan nanoparticles used in drug delivery system employing chemometric technique. Iran J Pharm Res 14: 665-675.
32. Talab AS, Hussein A, Kamil MM, Mostafa S, Hegazy NA, et al. (2024) Synthesis and characterization of chitosan nanoparticles from some crustacean wastes. Egypt J Chem 67: 23-42.
33. Andrew EC, Grace EA, Chinemerem OE, Emeka OE (2025) Mini review on the morphological and microanalysis characterization of chitosan nanocomposites using scanning electron microscopy. Mathews J Pharm Sci 9: 1-6.
34. El-Naggar NE, Eltarahony M, Hafez EE, Bashir SI (2023) Green fabrication of chitosan nanoparticles using Lavendula angustifolia, optimization, characterization and in vitro antibiofilm activity. Sci Rep 13: 11127.
35. Clark GL, Smith AF (2002) X-ray diffraction studies of chitin, chitosan, and derivatives. J Phys Chem 40: 863-879.
36. Sonin D, Pochkaeva E, Zhuravskii S, Postnov V, Korolev D, et al. (2020) Biological safety and biodistribution of chitosan nanoparticles. Nanomaterials 10: 810.
37. Zoe LH, David SR, Rajabalaya R (2023) Chitosan nanoparticle toxicity: A comprehensive literature review of in vivo and in vitro assessments for medical applications. Toxicol Rep 11: 83-106.
38. Riss TL, Moravec RA, Niles AL, Duellman S, Benink HA, et al. (2016) Cell viability assays. Assay Guidance Manual.
39. Kocabay S, Bahar MR, Tekin S, Akkaya R, Akkaya B (2021) Chemical and biological characterization of sulfated chitosan oligomer as heparin mimics. Polym Polym Compos 29: S1023-S1032.

40. Vigneshwari S, Gokula V (Year) Extraction and FTIR characterization of chitosan from Portunus pelagicus (Linnaeus, 1758) shell wastes.

41. Rehman HU, Cord-Landwehr S, Shapaval V, Dzurendova S, Kohler A, et al. (2023) High-throughput vibrational spectroscopy methods for determination of degree of acetylation for chitin and chitosan. Carbohydr Polym 302: 120428.